LAWRENCE
LIVERMORE
NATIONAL
LABORATORY

LLNL-JRNL-648674

Phase Diagram and Equation of State of Magnesium to High Pressures and High Temperatures

G. W. Stinton, S. G. MacLeod, H. Cynn, D. Errandonea, W. J. Evans, J. E. Proctor, Y. Meng, M. I. McMahon

January 21, 2014

Physical Review B

Disclaimer

Phase Diagram and Equation of State of Magnesium to High Pressures and High Temperatures

G. W. Stinton,[1] S. G. MacLeod,[2,3,4] H. Cynn,[5] D. Errandonea,[6]
W. J. Evans,[5] J. E. Proctor,[1] Y. Meng,[7] and M. I. McMahon[1,4]

[1]*SUPA, School of Physics and Astronomy, and Centre for Science at Extreme Conditions, The University of Edinburgh, EH9 3JZ, UK*
[2]*Atomic Weapons Establishment, Aldermaston, Reading, RG7 4PR, UK*
[3]*Institute of Shock Physics, Imperial College London, SW7 2AZ, UK*
[4]*Research Complex at Harwell, Didcot, Oxon, OX11 0FA, UK*
[5]*Lawrence Livermore National Laboratory, Condensed Matter and Material Division, Physics and Life Sciences Directorate, Livermore, CA 94551 USA*
[6]*Departamento de Fisica Aplicada - ICMUV, Universitat de Valencia, C/Dr. Moliner 50, Burjassot, E-46100, Valencia, Spain*
[7]*High Pressure Collaborative Access Team, Geophysical Laboratory, Carnegie Institution of Washington, Argonne, IL 60439, USA*

(Dated: January 17, 2014)

The phase diagram of magnesium metal has been investigated to 221 GPa at 300 K, and to 105 GPa at 4500 K, using a combination of x-ray diffraction and resistive and laser heating. The ambient pressure hcp structure is found to start transforming to the bcc structure at ∼45 GPa, with a large region of phase-coexistence that becomes smaller at higher temperatures. The bcc phase is stable to the highest pressures reached. The hcp-bcc phase boundary has been studied on both compression and decompression, and its gradient is found to be negative, and steeper than previous calculations have predicted. The laser heating studies extend the melting curve of magnesium to 105 GPa, and suggest that the melting temperature is more pressure dependent than previously reported. Finally, we observe some evidence of a new phase in the region of 10 GPa and 1200 K, where previous studies have reported a double-hexagonal close-packed (dhcp) phase. However, the additional diffraction peaks we observe cannot be accounted for by the dhcp phase alone.

INTRODUCTION

Magnesium (Mg) has been described as a nearly free-electron metal up to pressures of around 100 GPa.[1] This, combined with interest in the pressure-driven transfer of electrons from the *sp*-band to the 3*d*-band as the energy gap between the two decreases, has led to a number of theoretical studies[2–9] up to 30 TPa. Experimental studies have been conducted at room temperature (RT) to only the relatively modest pressure of 158 GPa.[10]

On compression, there is a well-established phase transition in Mg between the ambient-pressure hexagonal close-packed (hcp) phase and the body-centred cubic (bcc) phase between 44 and 58 GPa, with a large region of phase co-existence.[11] There are no studies of this transition on decompression. The bcc phase is known to be stable to 158 GPa.[10] At higher pressures, there have been several computational predictions of transformations to a number of different phases, but the transition pressures vary greatly between different calculations. McMahan and Moriarty[12] predicted a transition to the face-centred cubic (fcc) structure at either 180 or 790 GPa, using, respectively, the generalised pseudopotential theory or the linear muffin-tin orbital method. Chavarria[5] predicted a transition to the same structure at 1260 GPa (1.26 TPa). Ahuja *et al.*[3] predicted that the simple cubic structure would be stable above 660 GPa, while Li *et al.*[13] predicted a transition to the fcc structure at 456 GPa, followed by a transition to a phase with a simple hexagonal structure at 756 GPa. Most recently, Pickard and Needs[8] predicted a still more complex series of transitions: fcc to simple hexagonal at 0.75 TPa, simple hexagonal to simple cubic at 1 TPa, and simple cubic to orthorhombic at 30 TPa, where concentrations of electrons act as anions. However, none of these post-bcc phases have been observed experimentally.

At ambient pressure the hcp phase of Mg is stable up to the melting point at 923 K, and it is thus the only group-II metal not to melt from the bcc phase at ambient pressure. Kennedy and Newton[14] and Errandonea[15] determined the melting curve by resistivity measurements up to 12 GPa. Laser-heating experiments conducted by Errandonea *et al.*[16] agree with these measurements and reported that the melting temperature of Mg increases at around 45 K/GPa until 40 GPa[17] at which point the gradient decreases such that by 70 GPa the melting temperature is almost pressure independent. This nearly flat region in the melt curve is characteristic of alkali, rare earth and some transition metals above bcc phases.[16] There have been a number of *ab initio* calculations performed to determine the nature of the hcp-bcc phase boundary,[2,4,6,13] and these all show a negative slope, with the liquid-bcc-hcp triple point calculated to lie between 4 GPa and 1200 K[2] and 20 GPa and 1750 K.[13] Shock-compression studies along the Hugoniot[18] suggested the existence of a phase transition at 26.2(1.3) GPa and 900 K, which correlates well with the hcp-bcc phase boundary calculated by Moriarty and Althoff.[4]

X-ray diffraction, coupled with resistive heating, was used to determine the phases of Mg up to 18.6 GPa and 1527 K by Errandonea *et al.*[19] Above 1200 K, the (002) diffraction peak of the hcp phase was observed to split, and two new diffraction peaks emerged. The resulting diffraction pattern could be indexed by doubling the crystallographic *c*-axis of the hcp phase to give a double-hexagonal close-packed (dhcp) phase. This metastable phase was recoverable back to RT at 8.05 GPa. The phase boundary between the hcp and dhcp phases was found to have a negative gradient, opening the possibility that the hcp $\rightarrow$ dhcp transition may occur at room temperature at higher pressures. However, the stability field of the dhcp phase is still unknown. Errandonea *et al.*[19] found no transition to the bcc phase up to $\sim$18 GPa at $>$ 1100 K and $\sim$10 GPa and 1527 K, in disagreement with most previous calculations, except those of Li *et al.*[13] and the generalised gradient approximation calculations of Mehta *et al.*[6] which predicted the transition to the bcc phase only at higher pressures/temperatures. The most recent metadynamics calculations of Yao and Klug[9] addressed the relative stabilities of the hcp, dhcp and bcc phases both at room and elevated temperatures. While no stability range was found for the dhcp phase at RT, calculations at 15 GPa and 500 K revealed structural transformations back and forth between the hcp, dhcp, and bcc structures. The authors suggested that these structural fluctuations are driven by kinetics, and that the experimental observation of the dhcp structure is because it is much more energetically favourable than the bcc structure at $\sim$15 GPa.[9]

Despite much previous study, therefore, there still remain a number of inconsistencies between the observed and calculated behaviour of Mg. To address and resolve these, and to more fully explore the phase diagram of Mg, we have made a series of x-ray diffraction studies using diamond anvil cell experiments and different heating techniques. We have extended the room temperature compression of Mg up to 221 GPa, with the aim of looking for a transition from the bcc phase, and to provide a more accurate determination of the equation of state of the high-pressure bcc phase. In the second series of experiments, resistive heating of samples was carried out to 800 K and to pressures around 75 GPa with the aim of both accurately locating the phase boundary between the hcp and bcc phases, and determining the region of co-existence of the two phases on both compression and decompression. In the final series of experiments, laser-heating of samples in pressure cells was used to determine the onset of melting, to investigate the stability field of the dhcp phase, and to explore the high-temperature, high-pressure region of the phase diagram to look for further phases.

EXPERIMENTAL DETAILS

Three types of diamond anvil cell loading were made to address the three different types of experiment required. For the RT compression experiments to 221 GPa, two Boehler-Almax[20] type diamond anvil cells (DACs), henceforth referred to as cells 1 and 2, equipped with bevelled diamonds and rhenium gaskets, were loaded with Mg powder of 99.999% purity purchased from Aldrich Chemicals. No pressure transmitting medium (PTM) was used. Powder angle-dispersive x-ray diffraction (ADXRD) data were collected on compression using the HPCAT (High Pressure Collaborative Access Team) beamline at the Advanced Photon Source (APS), Argonne National Laboratory, Chicago, USA, using a wavelength of 0.398 Å and an x-ray beamsize of 5 μm in diameter. Cell 1 was loaded with micron-sized pieces of both copper (Cu) and tantalum (Ta) as pressure markers. Data from cell 1 were collected to 207 GPa. Cell 2 contained only Ta as a pressure marker. The pressure on cell 2 was increased first at the Diamond Light Source, but the relatively large x-ray beamsize (20 μm) meant that the diffraction patterns were heavily contaminated by diffraction peaks from the rhenium gasket. However, after increasing the pressure to close to 200 GPa, data with less intense gasket diffraction peaks were subsequently collected from cell 2 from 200 up to 221 GPa at the APS. Unfortunately, at this pressure, the anvils failed, terminating the experiment.

For the resistive heating part of this study, a preliminary series of measurements were carried out using a gas-membrane driven diamond anvil cell[21] with 250 μm culets at beamline 16-IDB at the APS using a incident x-ray wavelength of 0.398 Å. Cu powder was used as the pressure marker, and no pressure transmitting medium was used so as to prevent chemical reactions at high temperatures. The sample was heated using an external 650 W resistance heater (Watlow Ltd) wrapped around the outside of Lawrence Livermore National Laboratory (LLNL)-designed DACs inside a custom-designed vacuum vessel.[21] The sample pressure was adjusted using a gas-membrane system, and the temperature was measured using a K-type thermocouple attached to one of the diamond anvils, close to the gasket. Five further gas-membrane cells with either 250 and 300 μm culets were loaded and x-ray diffraction experiments were carried out on the I15 beamline at the Diamond Light Source (DLS) using an incident x-ray wavelength of 0.414 Å.

For the laser-heating measurements, pieces of 8 μm-thick Mg foil (99.999% purity, Aldrich Chemicals) were loaded between insulating layers of approximately the same thickness of MgO, into 12 Boehler-Almax cells equipped with diamonds with culet diameters ranging between 150 and 300 μm. Cu powder was included with the sample as a pressure marker, but sample pressures were determined from the equation of state of MgO as it was present in every diffraction image. Simultaneous laser-heating and x-ray diffraction was carried out on the HP-

CAT beamline at the APS using an x-ray wavelength of 0.620 Å and a beam diameter (FWHM) of 5 μm. Double-sided heating of the sample was achieved using two 100W YLF fiber lasers and temperatures were measured separately from both sides with an imaging spectrograph[22] and a PIXIS 400BR CCD. The laser heating spot size was approximately 20 μm (flat top area), significantly larger than the x-ray beam size. With the mirror pinhole setup,[23] the alignment of heating, temperature measurement and ADXRD spots can be directly monitored to ensure meaningful measurement results.

In all four sets of experiments, the 2-dimensional diffraction patterns were collected on either a MAR CCD (for laser heating at HPCAT) or a MAR345 image plate (resistive heating at HPCAT, and all studies at I15) and integrated azimuthally using Fit2d.[24] The resulting 1-dimensional diffraction profiles were analysed by Le Bail fitting[25] of the whole profiles using the TOPAS Academic package,[26] or by analysis of the *d*-spacings of individual diffraction peaks.

The pressure of the RT cell 2 was determined from the Ta pressure marker using the equation of state (EoS) determined by Cynn and Yoo.[27] The pressure of cell 1, and that of the DACs used in the resistive heating experiments, was determined from the Cu pressure marker in the sample chamber using the Cu EoS of Cynn.[28] Very few of the laser-heating diffraction images contained diffraction peaks from the Cu pressure marker, due to the small beam size and the need to position the laser and x-ray beam in places where good laser coupling could be achieved. Therefore, the MgO thermal insulation in the pressure chamber was used as the pressure calibrant. The pressure was determined from this using the EoS of Speziale *et al.*,[29] which accounted for both compression and changing temperature. In determining the pressure from the MgO, its temperature was assumed to be equal to the temperature inferred using pyrometry, that is, the temperature of the Mg-MgO interface. Axial temperature gradients are present in the MgO, with the MgO in contact with the diamond anvil being cooler than that in contact with the sample. A temperature difference of 1000 K corresponds to a pressure difference of approximately 7 GPa.[30] Upon heating, the integrated diffraction peaks from the MgO are noticeably broader than those from the sample. The additional width of the MgO peaks suggests a temperature gradient of around 500 K at a sample temperature of 1000 K, rising to around 700 K at a sample temperature of 2500 K. The stated pressures may thus be systematically 3-6 GPa too high, with the higher discrepancies at the higher temperature and higher pressure region of the phase diagram.

EXPERIMENTAL RESULTS

Room Temperature Compression and Equation of State

In addition to the two DACs specifically prepared to measure the RT compression beyond 200 GPa (cells 1 and 2), one of the gas-membrane DACs used for resistive heating (henceforth labelled cell 3) was first pressurised at RT to 78.1 GPa, before being decompressed to 32.7 GPa, in order to study the bcc-to-hcp transition on decompression. Cell 3 contained no pressure transmitting medium. On pressure increase, the onset of the phase transition[10,11,31] between the hcp and bcc phases was observed at 45.5(15) GPa at the lower limit of the transition pressure range of 50(6) GPa reported by Olijnyk and Holzapfel.[11] There are two likely reasons for this. Firstly, the absence of a PTM in the cell, the lack of which is known to reduce the pressure at which phase transitions are observed. Secondly, although the first evidence of the bcc phase in cell 3 was initially observed at 45.5(15) GPa, the diffraction peaks from the bcc phase remain very weak up to 53.4 GPa, as shown in Figure 1 (the only visible peak has an intensity between 3 and 8% of the strongest peak from the hcp phase over this pressure range). The weakness of the bcc peaks may have rendered them unobserved in the noisier data of Olijnyk and Holzapfel.

On further pressure increase in cell 3, we observed a large region of phase co-existence of the bcc and hcp phases, as previously reported,[11] such that single-phase diffraction profiles from the bcc phase were observed only above 61.1(11) GPa. In cell 1, we observed a considerably smaller co-existence region, with the bcc phase emerging at 49.9(19) GPa and single-phase patterns were observed above 57.7(18) GPa. On decompression of cell 3 from 78.1 GPa, the reverse bcc-to-hcp transition was found to start at 44.9(13) GPa and single-phase profiles of the hcp phase were observed only below 36.0(9) GPa.

After obtaining single-phase profiles of the bcc phase, the sample pressures in cells 1 and 2 were increased to maximum pressures of 207 GPa and 221 GPa, respectively. No further phase transitions were observed, and the bcc phase was found to be stable at RT to this maximum pressure, with no visible rhombohedral or tetragonal distortions, such as those found in vanadium.[32] The RT compressibility of the hcp and bcc phases on both pressure increase and decrease, as obtained from the samples in cells 1, 2 and 3, is shown in Figure 2. From mixed-phase profiles obtained between 47 and 57 GPa, the volume change ($\Delta V/V_0$) at the hcp-to-bcc transition is determined to be 0.45(18)% (see inset to Figure 1), in excellent agreement with the volume difference of 0.4(4)% reported by Nishimura *et al.*[10]

The compressibilities of the hcp and bcc phases were fitted with two separate Vinet[33] equations of state (EoS) using the EOSFIT package.[34] For comparison with previous studies,[7,10,19] the same data were also fitted

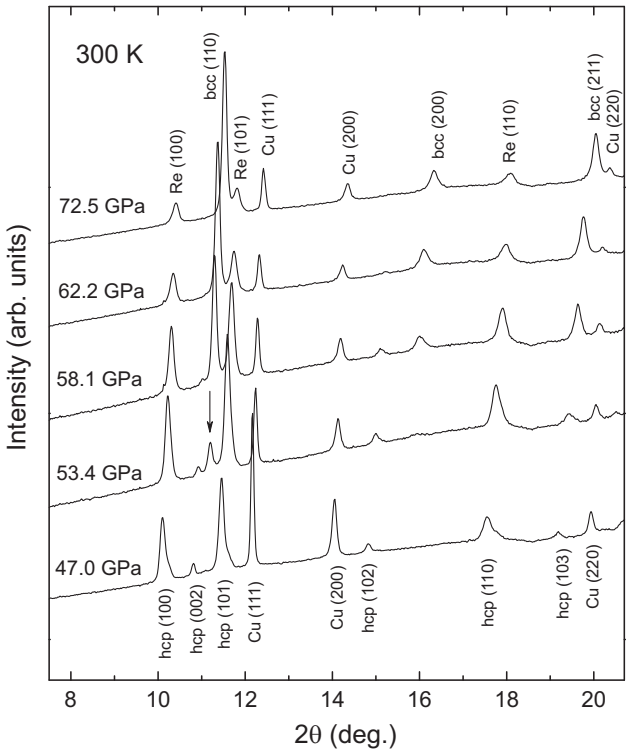

FIG. 1. Diffraction profiles collected from Mg on compression from 47.0 GPa to 72.5 GPa at RT, showing the onset of the hcp-to-bcc transition and the extended pressure range over which mixed-phase profiles are observed. The arrow above the 53.4 GPa pattern shows the appearance of the (110) reflection from the bcc phase. Diffraction peaks from the rhenium (Re) gasket in the 72.5 GPa profile are labeled.

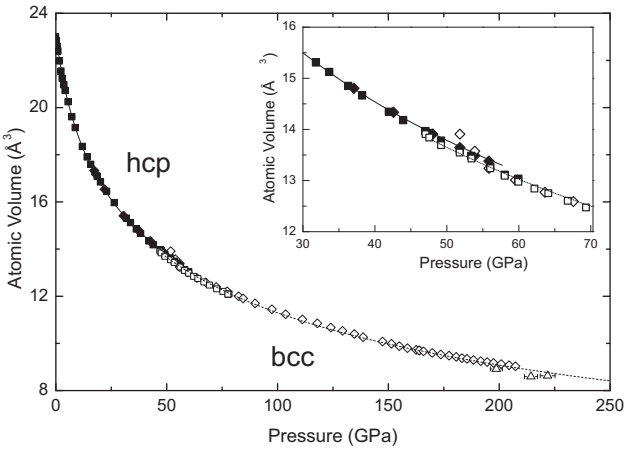

FIG. 2. The atomic volume of Mg as a function of pressure to 221 GPa, as obtained from cells 1, 2 and 3 (see main text for descriptions of each). Data points from the hcp phase are shown using solid symbols, while data from the bcc phase are shown using open symbols. Data from cells 1, 2 and 3 are plotted using diamonds, triangles and squares, respectively. The solid and dashed lines show the equations-of-state for the hcp and bcc phases, as determined from the current data, using the parameters given in Table I. Only error bars larger than the symbols used to plot the data are shown. The inset shows an enlarged view of the atomic volume at pressures between 40 and 60 GPa, and highlights the volume change at the hcp-to-bcc transition.

with a Birch-Murnaghan (B-M) EoS. V_0 of the hcp phase was fixed at its experimentally-determined value of 23.1495(8) Å^3 per atom. Determining the value of V_0 for the high-pressure bcc phase presented a greater problem, as this phase is not stable at ambient pressure, and refining a value for V_0 within EOSFIT showed that this parameter was correlated with both K_0 and K' at more than 98%. Liu *et al.*[7] calculated the relative volumes of the hcp and bcc phases at ambient pressure (at 0 K), and determined that the atomic volume of the bcc phase was 0.04% smaller than that of the hcp phase. This implies a value of V_0 for the bcc phase of 23.1398(8) Å^3 per atom, and K_0 and K' for the bcc phase were therefore refined with V_0 fixed at this value. The results of all of the EoS fits are shown in Table I. The bulk modulus determined here for the hcp phase is smaller than those determined previously,[7,10,19] although use of the B-M EoS gives slightly better agreement.

The EoS values determined for the bcc phase with a fixed V_0 are reasonably similar to those of Liu *et al.*[7], but disagree with the values of Nishimura *et al.*,[10]. However, the value Nishimura *et al.* determine for V_0 of the bcc phase is very small compared to that of the hcp phase. Allowing V_0 to refine, and using a B-M EoS, gave values for K_0 and K' of 45(8) GPa and 3.8(1), respectively, much closer to those of Nishimura *et al.* - see Table I. However, the large correlation between all parameters in this fit, together with the small value of V_0 (21.7(9) Å^3 per atom) and the large errors in the values, means we do not place much faith in these results.

RESISTIVE HEATING STUDIES

The six membrane-driven DACs used for the resistive heating studies were all initially pressurised to approximately 20 GPa, and then heated to 780, 700, 630, 480 and 400 K, with the sixth cell being compressed at RT for comparison. The measurements at 700 K were carried out at the APS, as previously described, and the rest at the Diamond Light Source. For each cell, the aim was to start with the sample being single-phase hcp, and then compress each of them at a fixed temperature through any mixed hcp-bcc phase region to obtain single-phase bcc samples before then decompressing the cells to investigate the reverse bcc-to-hcp transition, and thereby obtain information on the degree of hysteresis in the transition. The diffraction data obtained on compression and decompression at 700 K are shown in Figure 3, and the results obtained at the six different temperatures are summarised in Figure 4.

A number of conclusions can be drawn from these measurements. Firstly, the pressure at which the bcc phase

TABLE I. Results of fitting the experimental volumes of the hcp and bcc phases with Vinet and Birch-Murnaghan (B-M) equations of state, with the most recently published experimental and theoretical values for comparison.

			hcp		
	This Study	This Study	Nishimura *et al.*[10]	Errandonea *et al.*[19]	Liu *et al.*[7]
EoS	Vinet	B-M	B-M	B-M	B-M
V_0	23.1495(fixed)	23.1495 (fixed)	23.222(2)	23.05(15)	23.027
K_0	29.5(5)	30.4(5)	36.7(17)	36.8(30)	36.038
K'	4.88(9)	4.39(8)	3.7(4)	4.3(4)	3.831
			bcc		
	This Study	This Study	Nishimura *et al.*[10]	Liu *et al.*[7]	
EoS	Vinet	B-M	B-M	B-M	
V_0	23.1398 (fixed)	21.7(9)	19.95(7)	23.017	
K_0	28.9 (5)	45(8)	68.7(7)	35.997	
K'	4.80(4)	3.8(1)	3.47(4)	3.817	

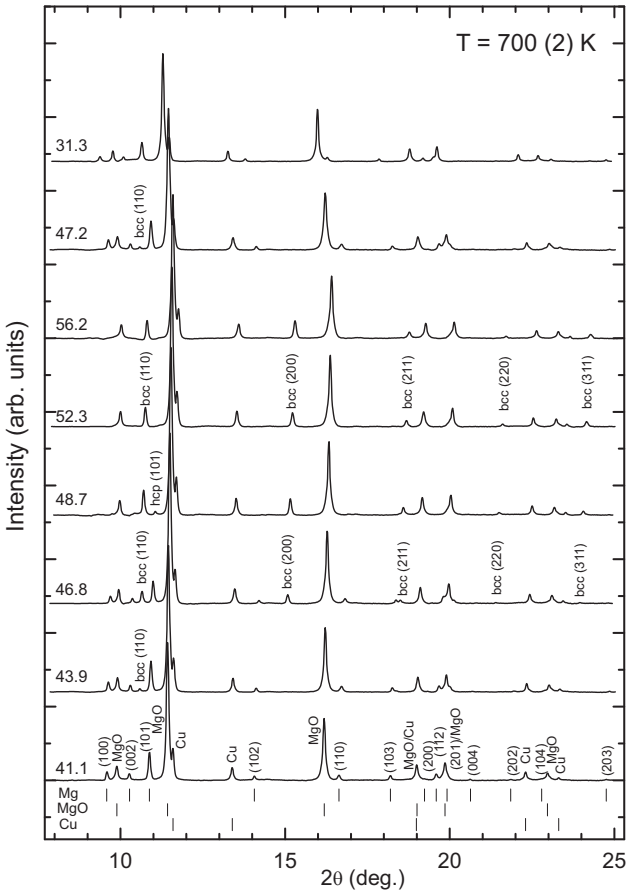

FIG. 3. Diffraction profiles collected on pressure increase from 41.1 to 56.2 GPa, and then back down to 31.3 GPa, at 700 K. The diffraction peaks from the Mg sample, MgO PTM and Cu pressure marker are identified with tickmarks beneath the bottom profile. Indices are given for the most intense diffraction peaks from each of the three materials. All diffraction patterns have had a smoothly varying background removed for clarity.

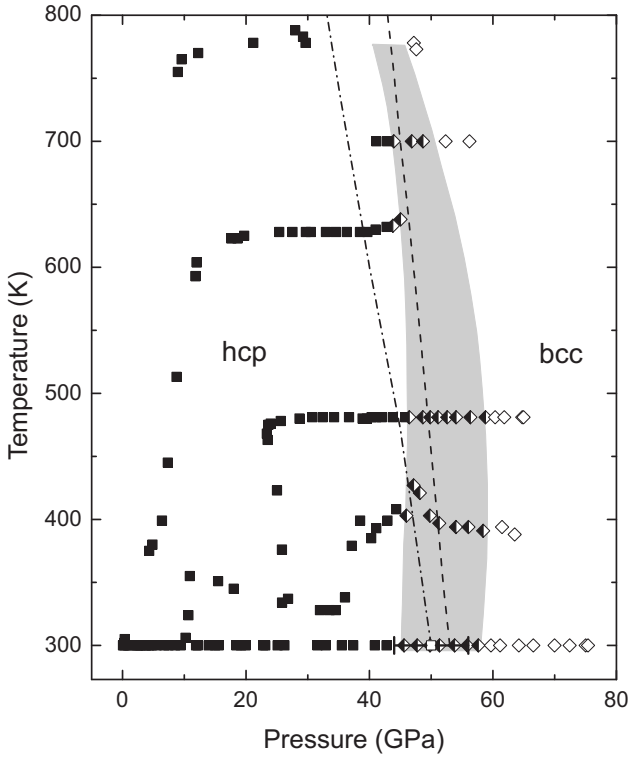

FIG. 4. The temperature dependence of the hcp-to-bcc phase transition pressure in Mg on compression. The *P*-*T* conditions at which single-phase hcp, mixed-phase hcp-bcc, and single-phase bcc profiles are observed are shown using filled, half-filled, and unfilled symbols, respectively. The unfilled square with error bars at 50 GPa and 300 K is the hcp-bcc phase transition pressure reported by Olijnik and Holzapfel[11]. The dot-dashed and dashed lines highlight the phase boundaries calculated by Moriarty and Althoff[4] and Mehta *et al.*[6], respectively, and the grey region shows the mixed-phase region determined in the current study.

first appears on compression increases slightly with increasing temperature, from 46.1(8) GPa at 400 K to 46.8(6) GPa at 700 K. However, the pressure at which the phase transition to the bcc was completed demonstrates a more dramatic change, dropping from ∼61 GPa between 300 and 480 K to 55(2) GPa at 700 K. Unfortunately, due to a sudden jump in pressure, it was not possible to obtain accurate transition pressures on compression from the sample at 780 K. However, a single-phase bcc pattern was obtained at 52.0(3) GPa, demonstrating a further drop in the transition completion pressure with temperature increase above 700 K. This decrease in the size of the mixed-phase region with temperature is to be expected, as it becomes easier to overcome the kinetic barriers to reach whichever phase is more thermodynamically stable.

Problems with seizure of the piston-cylinders in the DACs on pressure decrease at high temperatures meant that sufficient measurements to determine the transition region on decompression were obtained at only two temperatures, 300 K and 780 K. The mixed-phase region on decompression both decreases in pressure, and becomes narrower, with increasing temperature, from between 44.9(15) GPa and 36.0(9) GPa at 300 K to between 40.3(3) GPa and 33.9(5) GPa at 780 K. The general decrease in transition pressure with temperature agrees with calculations of Moriarty and Althoff[4], and also Mehta *et al.*[6], both of whom predicted the hcp-bcc transition boundary to have a negative gradient. The gradient calculated by Moriarty and Althoff is more negative than we observe, while the phase transition line calculated by Mehta *et al.* lies within the mixed-phase region determined here.

The c/a axial ratio of the hcp phase is 1.623(2) at ambient conditions, within error the same as the value of 1.624 reported by Young.[35] On the addition of only 1 GPa at RT, the axial ratio drops to around 1.617 and remains close to this value until the phase transition to the bcc phase. Within the margin of error, heating has no effect on this ratio. The reduction to 1.617 with increasing pressure, and lack of any change with temperature, is in agreement with the results of Errandonea *et al.*[19]

LASER HEATING STUDIES

The 12 Boehler-Almax Plate DACs prepared for laser heating, as described above, were precompressed to a range of pressures between 5.7 GPa and 90 GPa prior to heating. For each pressure cell, diffraction patterns were collected continuously as the power of the two lasers was ramped manually from 0.3 W to 62 W, with the powers of the two lasers illuminating each side of the sample adjusted to minimize temperature differences. The exposure times for the diffraction patterns for each cell were different, and varied between 2 s and 10 s. For all samples, the laser power was increased until either the sample melted, as described below, or the onset of large fluctuations in the radiation emitted from the sample precluded further temperature measurements *via* spectroradiometry. The onset of these rapid fluctuations was accompanied by recrystallisation of the sample, as judged by the changes in the positions of Bragg peaks on the detector from exposure to exposure. This phenomenon appears to be similar to that observed by Lazicki *et al.* in their recent laser-heating studies of Be.[36]

Detecting the existence of molten Mg, and determining the temperature at which melting occurs, is challenging. It is generally accepted that the complete disappearance of crystalline Bragg scattering is an indicator of melting. While this is necessary, however, it is not sufficient, and the observation of a diffuse halo of scattering from the liquid is also required for definitive proof of melting. But, for weakly scattering samples such as Li[37] and Be,[36] diffuse scattering from the liquid has not been observed, even in relatively large, resistively-heated samples. In the current study, we were able to observe the disappearance of all Bragg scattering from the crystalline phases at clearly discernible temperatures, which we have interpreted as the melting temperature. However, above the melting temperature we were not able to obtain any measurable scattering from the liquid phase. In addition to the disappearance of all Bragg scattering, in many samples we were also able to observe the onset of rapid recrystallisation of the samples at clearly defined temperatures below that of the melting temperature. Similar behaviour has recently been reported in laser-heating diffraction studies of Be,[36] Mo[38] and Fe.[39] This recrystallisation behavior was evident from the rapid appearance and disappearance of single-crystal-like Bragg scattering, which was clearly distinguishable from the disappearance of the Bragg scattering at higher temperatures that we associated with melting. In some of the samples, the rapid-recrystallisation of the sample also produced rapid and very large fluctuations in the measured temperature, which precluded further studies at higher temperatures, and thus the determination of true melting in these samples.

During laser heating, the sample pressure in all cells increased, as determined from the equation of state of the MgO PTM.[30] Analysis of the ADXRD patterns collected from the laser-heated samples revealed clear existence of two different phases below the melting curve, the hcp and bcc phases observed at RT, and some evidence of a third in the vicinity of 6 GPa and 1200 K, which is shown in Figure 5. This is the same region of the phase diagram in which Errandonea *et al.*[19] reported the existence of a phase with a double-hexagonal close-packed (dhcp) structure. The diffraction patterns obtained in the vicinity of 6 GPa and 1200 K contain some of the features expected from the dhcp structure, such as the appearance of the (103) and (105) reflections (as indexed using the dhcp structure). However, there are also two additional diffraction peaks at d-spacings of 2.24 Å and 1.40 Å, which are explained by neither the hcp or dhcp phase. These two peaks were not observed by Errandonea

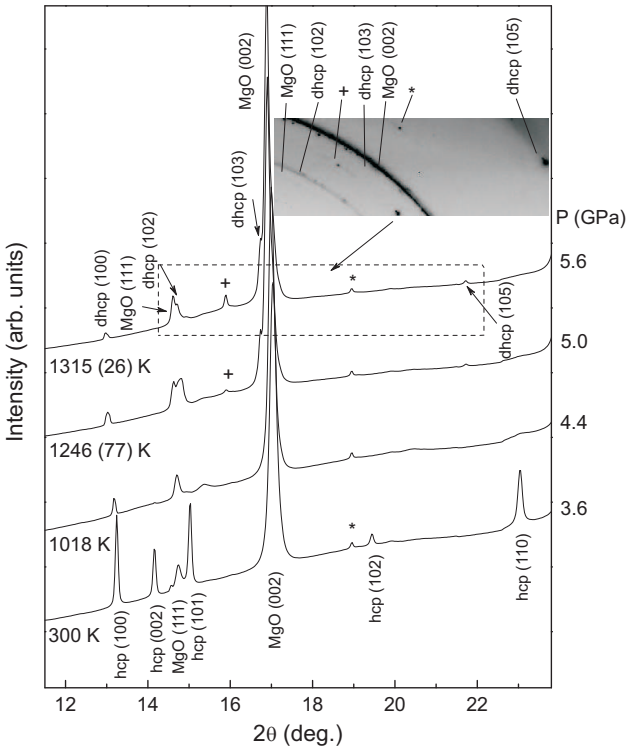

FIG. 5. Integrated diffraction patterns obtained on laser heating Mg from 300 K to 1315 K at 3.6 to 5.6 GPa. Two diffraction peaks, which can be indexed as the (103) and (105) peaks from a dhcp structure, appear at 1246(77) K, and are indexed in the highest-temperature profile. Two additional reflections, not fitted by the dhcp structure, appear at 15.9° (2.24 Å) and 25.6° (1.40 Å), and the lowest-angle of the two peaks is highlighted with a + symbol. The inset shows part of the 2D diffraction image collected at 1315 K, illustrating the spotty texture of the sample peaks.

et al.[19] The texturing evident in the Debye-Scherrer (D-S) rings of the two non-dhcp reflections matched that of the diffraction rings from the sample, and these D-S rings underwent the same process of recrystallisation as the other sample rings. All of the additional peaks are still observed after the sample was cooled to RT, as observed previously by Errandonea *et al.*[19] The evidence is therefore that the two non-dhcp peaks do come from the sample. Unfortunately, attempts to index all of the observed diffraction peaks as coming from a single phase were unsuccessful, and we cannot therefore make any definitive statement in the existence, or otherwise, of the dhcp phase. Only the lowest-pressure of our twelve samples showed any evidence of this phase, and further detailed investigations of this region of the phase diagram are required. The relevant *P*-*T* conditions are reachable using resistive microheaters, which should provide better quality, definitive, data.

As observed both at RT and in the resistive-heating studies, mixed-phase diffraction profiles containing both the hcp and bcc phases were found across a wide region of *P*-*T* space during the laser-heating studies. The pressure at which the bcc phase is first observed continues to decrease with increasing temperature, reaching 36 GPa at 1630 K. The bcc-hcp phase line is thus more vertical at higher temperatures than those calculated by Moriaty and Althoff, and Mehta *et al.*, and we can estimate that the hcp-bcc-liquid triple point is around 25 GPa and 2100 K. All of the present results are combined with previous studies of transitions and melting of Mg into the comprehensive phase diagram of Mg to 105 GPa shown in Figure 6.

The bcc phase was clearly observed at both 89 GPa & 3980 K and 97 GPa & 4320 K, above the melting line of Errandonea *et al.*[16] A modification to the melting curve to account for these points is given in Figure 6. There are two possible reasons for the discrepancy in the two data sets, where there is a much less severe curvature in the region of 40 to 60 GPa in this work. Firstly, in Errandonea *et al.* the speckle method was used to detect melting. Using this method, the liquid phase was detected by the movement observed at the Mg surface after the onset of melting. The detection of this movement becomes more difficult as pressure increases (among other things because the viscosity of the liquid increases). Also recrystallisation may occur significantly below the melting temperature, leading to movement that is similar to the motion from melting. As a consequence of this, the melting temperature may have been underestimated beyond 60 GPa. Secondly, in laser heating there are axial temperature gradients in the sample, even when using double-sided heating. The center of the sample will therefore be cooler than the surface, and the temperature is measured from the surface. It is thus possible that even after the onset of melting at the surface, the centre of the sample is still a solid and still diffracting. It should be noted that the disagreement with the data of Errandonea *et al.* is primarily due to a single point in their work at 87 GPa and 3480 K. The upper part of the error bars of the rest of the data gives reasonable agreement with the lowest part of the current data.

THERMAL EQUATION OF STATE

The atomic volumes of the hcp and bcc phases with respect to both pressure and temperature were fitted separately to a Vinet EoS modified to account for thermal effects, as described by Angel.[34] The EoSs of both phases used all the data from the RT, resistive and laser heating parts of this work in combination. The values of V_0, K_0 and $K\prime$ for both phases were fixed at the values determined from the RT measurements, as shown in Table I, and the thermal expansion, α_0, for the hcp phase was fixed at 2.5×10^{-5} K^{-1}.[41] The remaining parameters, α_1 and $\partial K_0/\partial T$ for both phases, and α_0 for the bcc phase, were freely refined using EOSFIT.[34] The results are shown in Table II.

In comparison to the thermal expansion constants for the hcp phase determined by Errandonea *et al.*, our value

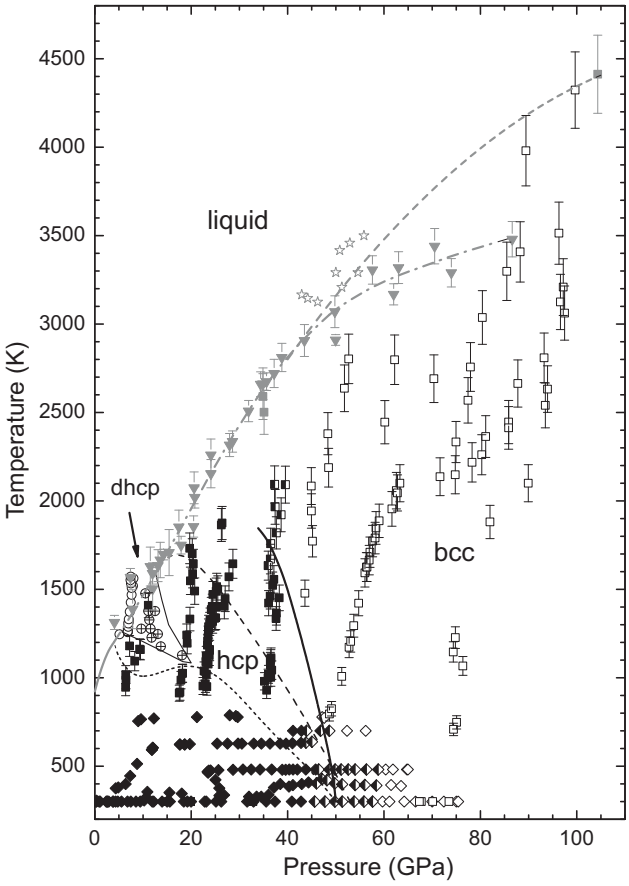

FIG. 6. The P - T phase diagram of Mg to 105 GPa and 4500 K. hcp-phase points are shown in black, bcc-phase points are shown using unfilled symbols and mixed-phase points are shown using half-filled symbols. Points where melting is observed are plotted with grey-filled symbols. Data plotted with square symbols are from the laser-heating portion of this study, and diamonds symbols plot the resistive heating data. The circular symbols with crosses around 15 GPa and 1300 K are those labeled dhcp in Errandonea *et al.*,[19]; points where extra diffraction peaks were observed in this study are shown as open circles. The data plotted with stars near 50 GPa and 3500 K show the melt points from Urtiew and Grover.[40] Grey, downward-pointing triangles show the melting points from Errandonea *et al.*,[16] with the grey dot-dash line showing the fit to these data from the same work. The grey dashed line at higher temperature is an extension to the Errandonea *et al.* melt line above 50 GPa, extrapolated to give the best agreement with the present data. The black lines at lower pressures show the hcp-bcc phase boundaries of Moriarty and Althoff[4] (dotted) and Mehta *et al.*,[6] (dashed), with the solid black line showing the phase boundary determined in the current study.

of α_1 for the hcp phase is larger, suggesting a stronger temperature dependence of the thermal expansion than previously thought. We find the bcc phase to have both a smaller thermal expansion, and a smaller first derivative, than the hcp phase. This tendency to expand less relative to the hcp phase with increasing temperature should make the bcc phase more favourable at higher temperatures under pressure; this supports the negative slope of the phase transition. Finally, the smaller (in an absolute sense) value of $\partial K_0/\partial T$ for the hcp phase implies that the effect of temperature on the bulk modulus is smaller than previously determined.

TABLE II. Results of fitting the experimental volumes with a Vinet EoS, with the most current published experimental values for comparison.

	bcc	hcp	Errandonea *et al.*[19]
α_0 ($\times 10^{-5}$K^{-1})	2.2(6)	2.5 (fixed)	2.5 (fixed)
α_1($\times 10^{-8}$K^{-2})	4.7(4)	8.1(5)	2.3(2)
$\partial K_0/\partial T$ GPa K^{-1}	−0.0052 (4)	−0.0073 (5)	−0.0208 (9)

CONCLUSIONS

The phase diagram of magnesium has been extended to 221 GPa at room temperature, and to 105 GPa at 4500 K. At 300 K, the onset of the hcp to bcc phase transition is observed at 46-50 GPa, probably dependent on how hydrostatic the sample in each cell is. The bcc phase was found to be stable to 221 GPa. The extended pressure range of our measurements has enabled us to determine a more accurate EoS for the bcc phase. From our resistive heating studies, the gradient of the hcp-bcc phase boundary has been determined experimentally for the first time, and is of the order of -130 K/GPa. While the negative gradient is in agreement with the theoretical predictions of Moriarty and Althoff, and Mehta *et al.*,[4,6] the experimental phase boundary is noticably more vertical than the results of the calculations.

Our new melting temperature data to 100 GPa do not reproduce the previously-reported sharp change in the slope of the melting curve around 50 GPa. Rather, we observe only a slight change in the gradient with pressure, such that at 100 GPa the melting temperature is 4300 K, some 800 K higher than previously reported. This difference in temperature probably results from the different methods used to detect the onset of melting.

Finally, the additional diffraction peaks reported by Errandonea *et al.*[19] in the vicinity of 10 GPa and 1300 K are also observed in the current study, and, as in that study, these peaks are found to remain on cooling back to room temperature. However, we cannot assign all of the peaks to the dhcp structure suggested by Errandonea *et al.*[19] The origin of these peaks, and whether they come from a further phase of Mg, is therefore still unknown and a further detailed study of the Mg phase diagram in the region of 10 GPa and 1300 K is still required.

ACKNOWLEDGEMENTS

HPCAT is supported by CIW, CDAC, UNLV and LLNL through funding from DOE-NNSA, DOEBES and NSF. APS is supported by DOE-BES, under Contract No. DE-AC02-06CH11357. This work was performed under the auspices of the U.S. Department of Energy by Lawrence Livermore National Laboratory in part under Contract W-7405-Eng-48 and in part under Contract DE-AC52-07NA27344. ©British Crown Owned Copyright 2014/AWE. Published with permission of the Controller of Her Britannic Majesty's Stationery Office. MIM is grateful to AWE Aldermaston for the award of a William Penney Fellowship. DE thanks the financial support of the Spanish MINECO under Grants No. MAT2010-21270-C04-01 and No. CSD2007-00045. We would like to thank Heribert Wilhelm and Annette Kleppe at I15 at the Diamond Light Source for their support.

[1] A. K. McMahan, Physica B & C **139**, 31 (1986).
[2] J. D. Althoff, P. B. Allen, R. M. Wentzcovitch, and J. A. Moriarty, Phys. Rev. B **48**, 13253 (1993).
[3] R. Ahuja, O. Eriksson, J. M. Wills, and B. Johansson, Phys. Rev. Lett. **75**, 3473 (1995).
[4] J. A. Moriarty and J. D. Althoff, Phys. Rev. B **51**, 5609 (1995).
[5] G. R. Chavarria, Phys. Lett. A **336**, 210 (2005).
[6] S. Mehta, G. D. Price, and D. Alfè, J. Chem. Phys. **125**, 194507 (2006).
[7] Q. Liu, C. Fan, and R. Zhang, J. App. Phys. **105**, 123505 (2009).
[8] C. J. Pickard and R. J. Needs, Nat. Mater. **9**, 624 (2010).
[9] Y. Yao and D. D. Klug, J. Phys.: Condens. Matter **24**, 265401 (2012).
[10] N. Nishimura, K. Kinoshita, Y. Akahama, and H. Kawamura, in *Proc. The 20th AIRAPT Int. Conf. on High Pressure Science and Technology* (Mineralogical Soc. America, Karlsruhe, Germany, 2005), pp. T10–P054.
[11] H. Olijnyk and W. B. Holzapfel, Phys. Rev. B **31**, 4682 (1985).
[12] A. K. McMahan and J. A. Moriarty, Phys. Rev. B **27**, 3235 (1983).
[13] P. Li, G. Gao, Y. Wang, and Y. Ma, J. Phys. Chem. C **114**, 21745 (2010).
[14] G. C. Kennedy and R. C. Newton, *Solids Under Pressure* (McGraw-Hill, New York, USA, 1963).
[15] D. Errandonea, J. Appl. Phys. **108**, 033517 (2010).
[16] D. Errandonea, R. Boehler, and M. Ross, Phys. Rev. B **65**, 012108 (2001).
[17] There is a typographical error in Ref. 16, where the gradient of the melting curve is stated to be 6 K/GPa. The true value of 45 K/GPa is clear from Fig. 1 of Ref 16.
[18] D. Milathianaki, D. C. Swift, J. Hawreliak, B. S. El-Dasher, J. M. McNaney, H. E. Lorenzana, and T. Ditmire, Phys. Rev. B **86**, 014101 (2012).
[19] D. Errandonea, Y. Meng, D. Hausermann, and T. Uchida, J. Phys.: Condens. Matter **15**, 1277 (2003).
[20] R. Boehler and K. D. Hantsetters, High Pressure Res. **24**, 391 (2004).
[21] Z. Jenei, H. Cynn, K. Visbeck, and W. J. Evans, Review of Scientific Instruments **84**, 095114 (2013).
[22] G. Y. Shen, M. L. Rivers, Y. B. Wang, and S. R. Sutton, Rev. Sci. Instrum. **72**, 1273 (2001).
[23] R. Boehler, H. G. Musshoff, R. Ditz, G. Aquilanti, and A. Trapananti, Rev. Sci. Instrum. **80**, 045103 (2009).
[24] A. P. Hammersley, S. O. Svensson, M. Hanfland, A. N. Fitch, and D. Hausermann, in *4th Workshop of the IUCr High Pressure Group on Synchrotron and Neutron Sources* (High Pressure Res., KEK, Japan, 1996), vol. 14, pp. 235–248.
[25] A. L. Bail, H. Duroy, and J. L. Fourquet, Mater. Res. Bull. **23**, 447 (1988).
[26] A. A. Coelho, *Topas Academic* (2007).
[27] H. Cynn and C. S. Yoo, Phys. Rev. B **59**, 8526 (1999).
[28] H. Cynn, *Unpublished*.
[29] S. Speziale, C.-S. Zha, T. S. Duffy, R. J. Hemley, and H.-k. Mao, Journal of Geophysical Research: Solid Earth **106**, 515 (2001), ISSN 2156-2202.
[30] Y. Tange, Y. Nishihara, and T. Tsuchiya, J. Geophys. Res. **114**, B03208 (2009).
[31] F. Jona and P. M. Marcus, J. Phys.: Condens. Matter **15**, 7727 (2003).
[32] Y. Ding, R. Ahuja, J. Shu, P. Chow, W. Luo, and H. K. Mao, Phys. Rev. Lett. **98**, 085502 (2007).
[33] P. Vinet, J. Ferrante, J. H. Rose, and J. R. Smith, J. Geophys. Res. **92**, 9319 (1987).
[34] R. Angel, *Reviews In Mineralogy & Geochemistry*, vol. 41 (Mineralogical Soc. America, 2000).
[35] D. A. Young, *Phase Diagrams of the Elements* (University of California Press, 1990).
[36] A. Lazicki, A. Dewaele, P. Loubeyre, and M. Mezouar, Phys. Rev. B **86**, 174118 (2012).
[37] C. L. Guillaume, E. Gregoryanz, O. Degtyareva, M. I. McMahon, M. Hanfland, S. Evans, M. Guthrie, S. V. Sinogeikin, and H.-K. Mao, Nat. Phys. **7**, 211 (2011).
[38] D. Santamaria-Perez, M. Ross, D. Errandonea, G. D. Mukherjee, M. Mezouar, and R. Boehler, J. Chem. Phys. **130**, 124509 (2009).
[39] S. Anzellini, A. Dewaele, M. Mezouar, P. Loubeyre, and G. Morard, Science **340**, 464 (2013).
[40] P. A. Urtiew and R. Grover, J. Appl. Phys. **48**, 1122 (1977).
[41] Y. S. Touloukian, *A Physicist's Desk Reference: The Second Edition of the Physics Vade Mecum* (American Institute of Physics, New York, USA, 1989).